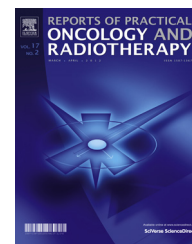


Available online at www.sciencedirect.com

ScienceDirect

journal homepage: <http://www.elsevier.com/locate/rpor>

Technical note

Evaluation of cone-beam computed tomography image quality assurance for Vero4DRT system



Hideharu Miura^{a,*}, Shuichi Ozawa^{a,b}, Masahiro Hayata^a,
Shintarou Tsuda^a, Tsubasa Enosaki^a, Kiyoshi Yamada^a,
Yasushi Nagata^{a,b}

^a Hiroshima High-Precision Radiotherapy Cancer Center, Japan

^b Department of Radiation Oncology, Institute of Biomedical & Health Science, Hiroshima University, Japan

ARTICLE INFO

Article history:

Received 17 May 2016

Received in revised form

9 September 2016

Accepted 2 December 2016

Keywords:

Vero4DRT

Cone-beam computed tomography

Quality assurance

Image-guided radiation therapy

ABSTRACT

We report the characteristics of quality assurance (QA) image for Vero4DRT system with a kilo-voltage (kV) cone-beam computed tomography (CBCT) capability to perform image-guided radiation therapy (IGRT). To acquire a set of CBCT, the kV source is rotated either 215° clockwise (CW) (tube 1 from 5° to 220° and tube 2 from 275° to 130°) or counterclockwise (CCW) (tube 1 from 85° to 230° and tube 2 from 355° to 140°). Image geometry, image uniformity, high/low contrast resolutions, and contrast linearity were measured with a Catphan 504 CT phantom (The Phantom Laboratory, NY). The comparison between measured and expected distances shows an excellent agreement. The CBCT for Vero4DRT system cannot perform a full 360° rotation, which leads to a loss in uniformity for image acquisition. Separations were observed for high-contrast resolution, with eight line pairs per centimeter corresponding to a gap size of 0.063 cm. For low-contrast resolution, the seventh largest hole was visible. This hole has a 4-mm diameter with 1.0% contrast level. We should check the contrast linearity compared with known value, even though it is out of range from the manufacturer manual.

© 2016 Greater Poland Cancer Centre. Published by Elsevier Sp. z o.o. All rights reserved.

1. Introduction

Image-guided radiation therapy (IGRT) has become a widely established standard in the treatment of cancer and plays an important role in improving the precision and accuracy of treatment delivery.^{1–3} An accurate patient setup is required as prescribed doses are very precisely delivered in stereotactic

body radiotherapy (SBRT), intensity modulated radiotherapy (IMRT), and volumetric modulated arc radiotherapy (VMAT) techniques; further, a high dose gradient exists out of planning target volume (PTV). IGRT is used for accurate patient setup which is required to improve precision and accuracy of treatment delivery. IGRT imaging strategies have utilized X-rays, ultrasound, and optical surface imaging (OSI).^{4,5} A

* Corresponding author at: Hiroshima High-Precision Radiotherapy Cancer Center, 3-2-2, Futabanosato, Higashi-ku, Hiroshima 732-0057, Japan. Fax: +81 082 263 1331.

E-mail address: miura@hiprac.jp (H. Miura).

<http://dx.doi.org/10.1016/j.rpor.2016.12.001>

1507-1367/© 2016 Greater Poland Cancer Centre. Published by Elsevier Sp. z o.o. All rights reserved.

cone-beam computed tomography (CBCT) with a kV-source and a flat-panel detector mounted onto the gantry of the linear accelerator is mostly used for IGRT. In the past few years, studies have been published regarding CBCT performance comparisons.^{6–8}

Vero4DRT (MHI-TM2000) system was recently developed by Mitsubishi Heavy Industries, Ltd., Japan (MHI) in collaboration with the Kyoto University and the Institute of Biomedical Research and Innovation (IBRI). The American Association of Physicists in Medicine (AAPM) Task Group (TG) 142 recommends daily, monthly and annual imaging quality assurance (QA) of IGRT.⁹ This report mentioned that for several reasons machine parameters can deviate from their baseline values, measured at the time of acceptance and commissioning. That is, the baseline data from acceptance testing by the vendor are recommended as a criteria for imaging QA. Currently, there has been no useful information published of Vero4DRT for CBCT image quality data.

In this paper, we report the characteristics of CBCT image QA for Vero4DRT system with kV-CBCT capability for performing IGRT. Image geometric, image uniformity, high/low contrast resolutions, and contrast linearity were measured.

2. Materials and methods

2.1. Vero4DRT

The characteristics of Vero4DRT system were already published^{10–14} (Fig. 1). Vero4DRT system has a high precision isocenter at the mechanical center of the gantry, which is shaped like an O-ring.¹⁴ The X-ray head with the gimbals can be rotated on the O-ring and moved to pan and tilt directions for dynamic tumor tracking (DTT). Meanwhile, the O-ring can be skewed around its vertical axis, removing the need to shift the treatment couch. Vero4DRT system has a dual kV

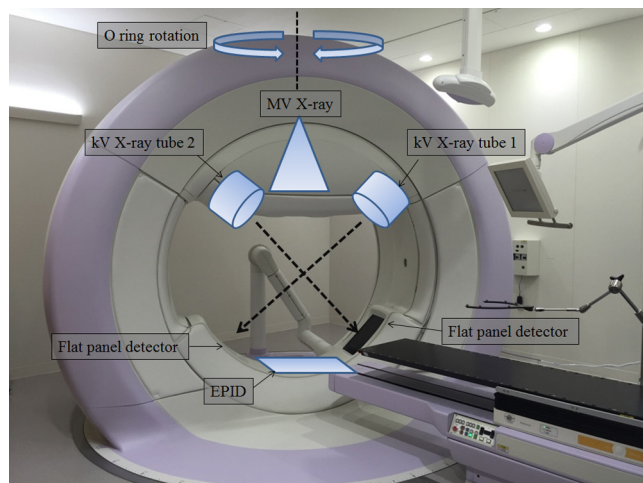


Fig. 1 – Vero4DRT system with the dual implementation of kV imaging system and electronic portal. The basic structure is the O-ring with a diameter of about 350 cm. The gantry is located inside the O-ring and can be rotated $\pm 180^\circ$ around the isocenter. The O-ring itself can be rotated $\pm 60^\circ$ around its vertical axis through the isocenter.

X-ray imaging subsystem attached to the O-ring at 45° from the megavoltage (MV) beam axis, an electronic portal imaging device (EPID), which are mounted on the O-ring-shaped gantry, and the kV CBCT also has imaging capability. The CBCT images are acquired using kV X-ray tube by rotating the gantry angle. To acquire a set of CBCT images the kV source is rotated either 215° clockwise (CW) (tube 1 from 5° to 220° and tube 2 from 275° to 130°) or counterclockwise (CCW) (tube 1 from 85° to 230° and tube 2 from 355° to 140°). It takes approximately 30 s to acquire the CBCT data by rotating 200° , as the O-ring rotation speed is limited to 7 deg/s.

2.2. Verification of the isocenter alignment of Vero4DRT system

The alignment of the isocenter of the kV imaging system and the MV beam is crucial for accurate patient positioning. The accuracy of the imaging device for target localization was estimated using a water-equivalent cube phantom ($130\text{ mm} \times 130\text{ mm} \times 130\text{ mm}$) with a 10-mm diameter steel ball fixed in the center of the phantom. Vero4DRT system needs to verify the isocenter position from 12 directions; performed in a similar way of a common linac system (e.g., Winston-Lutz test) before clinical use. This procedure cannot be skipped. Next, we verified the center position of the CBCT for daily QA. The results showed that the isocenters coincidence was good and within a range of 1.0 mm.

2.3. Image quality analysis

All the CBCT image QA can be performed using a Catphan 504 CT phantom (The Phantom Laboratory, NY), a well-established and validated QA tool that incorporates several modules for CT-QA.¹⁵ The uniformity, high/low contrast resolution, and Hounsfield Unit (HU) modules were used in this study. The alignment marks on the surface of the phantom were used to position the phantom at each imaging device with the in-room laser system. The phantom position alignment was checked using four wire ramps, which rise at 23° from the base to the top of the module. We separately measured the containing of each module. The phantom was centered, so that its physical center was at the treatment isocenter and one CBCT scan of the phantom. Using tubes 1 and 2, all modules were scanned for both CW and CCW directions. The X-ray parameters for the image acquisition were 120 kVp, 200 mA, and 10 ms. The reconstructed field of view (FOV) is a circle of 20 cm. The reconstruction matrix has a dimension of 512×512 and the slice thickness was 3.0 mm. The spatial resolution of the CBCT dataset had a voxel size of $0.39\text{ mm} \times 0.39\text{ mm} \times 3.00\text{ mm}$. For the image quality analysis, all the regions of interest (ROI) statistics were performed using the ImageJ software ver 1.49 (National Institute of Health, USA, <http://rsb.info.nih.gov/ij>).

2.4. Image geometric

The geometric CTP404 module consists of four holes (one with a Teflon pin). These 3-mm diameter holes are positioned 50-mm apart from their centers. By measuring from center to center, the image geometric of the CBCT can be verified.

2.5. Image uniformity

The uniformity CTP 486 module has a uniform disk to assess image noise and uniformity. Five square (3.0 cm × 3.0 cm) ROIs were assessed in the image center and peripheries (top, bottom, left, and right). The uniformity can be described by the Uniformity. It was defined as the maximum percentage difference between each of the peripheral areas and the central area:

$$\text{Uniformity} = \left| \overline{CT}_{\text{ROI, periphery}} - \overline{CT}_{\text{ROI, center}} \right|$$

where $\overline{CT}_{\text{ROI, periphery}}$ and $\overline{CT}_{\text{ROI, center}}$ are respectively the mean pixel value of the ROI at the four peripheral and center positions.

2.6. High-contrast resolution

The high-resolution CTP528 module has a 1 through 21 line pairs per centimeter (Lp/cm) high-resolution pattern. High-contrast resolution was evaluated using a modulation transfer function (MTF); a method reported by Droegge et al.¹⁶ and given by the following equation:

$$\text{MTF}(f) = \frac{\pi\sqrt{2}}{4} \cdot \frac{M(f)}{M_0}, f > \frac{f_c}{3}$$

where $M(f)$ refers to the standard deviation within a ROI (high-contrast modules). In the presence of noise, the measured value M' can be corrected to the noise effect, then:

$$M = \sqrt{M'^2 - N^2}$$

where N is the standard deviation of the CT image values within a “uniform” ROI.

M_0 is obtained by the following equation:

$$M_0 = \frac{|CT_1 - CT_2|}{2}$$

where CT_1 and CT_2 are the number of pixels of the CT values in the high-contrast module and in the water, respectively.

To qualitatively assess the spatial resolution, MTF values of 50% and 10% were calculated using the MTF curve data. The highest number of visible Lp was considered the spatial resolution in Lp/cm. The Lp visibility was determined by three independent observers.

2.7. Low-contrast resolution

The low-contrast CTP515 module consists of 27 contrast target discs arranged in three groups. The groups have nominal contrast of 1.0%, 0.5%, and 0.3% and decreasing diameters of 15, 9, 8, 7, 6, 5, 4, 3, and 2 mm. 1.0% contrast hole was used

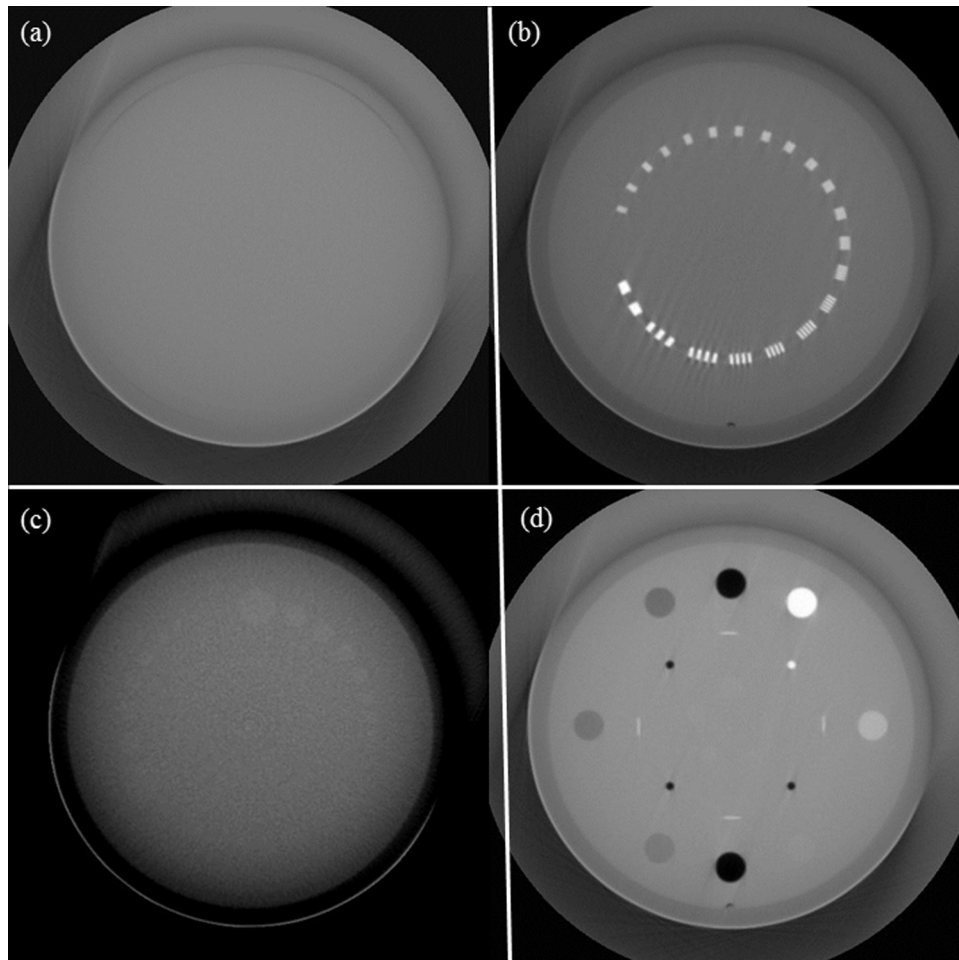


Fig. 2 – CBCT images of (a) image uniformity, (b) high-contrast resolution, (c) low-contrast resolution, and (d) Hounsfield Unit (HU) modules.

Table 1 – Performance of 4 acquisitions in distance values derived from four holes.

Angle (tube)	Upper right-upper left (mm)	Upper left-lower left (mm)	Lower left-lower right (mm)	Lower right-upper right (mm)
CW: 5°–220° (No.1)	49.9	49.9	50.1	50.1
CCW: 85°–230° (No. 1)	50.1	50.1	50.1	50.1
CW: 275°–130° (No. 2)	50.2	50.1	50.1	50.2
CCW: 355°–140° (No. 2)	50.1	50.1	50.1	50.1

CW, clock wise; CCW, counter clock wise.

Table 2 – Performance of 4 acquisitions in average Hounsfield Unit (HU) value and standard deviation (SD) values on each ROI derived from uniformity module.

Angle (tube)	Center	Top	Left	Bottom	Right
CW: 5°–220° (No. 1)	-128.7 ± 6.8	-139.2 ± 13.6	-174.0 ± 16.5	-165.4 ± 11.3	-148.6 ± 12.8
CCW: 85°–230° (No. 1)	-135.3 ± 6.5	-194.7 ± 21.6	-134.3 ± 9.6	-137.5 ± 7.4	-200.2 ± 19.8
CW: 275°–130° (No. 2)	-79.4 ± 5.7	-100.5 ± 13.7	-87.9 ± 8.9	-81.9 ± 6.1	-93.4 ± 11.4
CCW: 355°–140° (No. 2)	-74.8 ± 6.2	-100.7 ± 14.7	-91.5 ± 10.5	-76.2 ± 5.6	-91.0 ± 10.9

CW, clock wise; CCW, counter clock wise.

Table 3 – Performance of 4 acquisitions in image uniformity derived from uniformity module.

Angle (tube)	Top	Left	Bottom	Right
CW: 5°–220° (No. 1)	10.5	45.4	36.8	20.0
CCW: 85°–230° (No. 1)	59.4	1.0	2.2	64.9
CW: 275°–130° (No. 2)	21.1	8.5	2.5	14.0
CCW: 355°–140° (No. 2)	25.9	16.8	1.5	16.2

CW, clock wise; CCW, counter clock wise.

to evaluate low-contrast resolution. The hole visibility was determined by three independent observers.

2.8. Contrast linearity

The contrast linearity CTP404 module consists of seven different density materials (Air, PMP, LDPE, Polystyrene, Acrylic, Delrin and Teflon). For each material the mean values were measured in a circle with diameter of 1.0 cm. Measured values and CT values acquired with an Optima 580 W CT scanner (General Electric Company, Waukesha, WI) were compared to evaluate the contrast linearity.

3. Results

Fig. 2 shows the CBCT image dataset, which was obtained using a Catphan CT phantom.

3.1. Image geometric

Table 1 shows the results for distance measurement. The difference between the measured and expected distances was 0.11 ± 0.03 mm.

3.2. Image uniformity

Table 2 shows the average and standard deviation values at each ROI of the image.

Table 3 shows the image uniformity value at each ROI of the image.

3.3. High-contrast resolution

Table 4 shows the results for 50% and 10% MTF spatial resolution. For high-contrast resolution, the 8 Lp/cm corresponding to a gap size of 0.063 cm were observed with separation.

3.4. Low-contrast resolution

For low-contrast resolution, the seventh largest hole was visible. This hole has a 4-mm diameter with 1.0% contrast level.

3.5. Contrast-linearity

Table 5 shows the material measured mean values and expected HU value presented in the manufacturer manual.

Table 4 – Performance of 4 acquisitions in modulation transfer function (MTF) derived from high contrast resolution module.

Angle (tube)	50% MTF (mm ⁻¹)	10% MTF (mm ⁻¹)
CW: 5-220° (No.1)	0.39	0.77
CCW: 85- 230° (No.1)	0.38	0.74
CW: 275-130° (No.2)	0.37	0.75
CCW: 355-140° (No.2)	0.37	0.78

CW, clock wise; CCW, counter clock wise.

Table 5 – Performance of 4 acquisitions in average Hounsfield Unit (HU) values derived from HU module.

Material	CW: 5°–220° (No. 1)	CCW: 85°–230° (No. 1)	CW: 275°–130° (No. 2)	CCW: 355°–140° (No. 2)	Expected range
Air	–948.5	–946.8	–867.4	–902.0	–1046 to –986
PMP	–289.1	–299.4	–231.8	–239.5	–220 to –172
LDPE	–254.1	–204.2	–163.9	–162.3	–121 to –87
Polystyrene	–220.4	–165.1	–120.9	–114.3	–65 to –29
Acrylic	–73.8	–49.6	17.3	21.8	92 to 137
Delrin	145.0	110.8	203.2	216.1	344 to 387
Teflon	659.7	589.1	675.8	710.7	941 to 1060

CW, clock wise; CCW, counter clock wise.

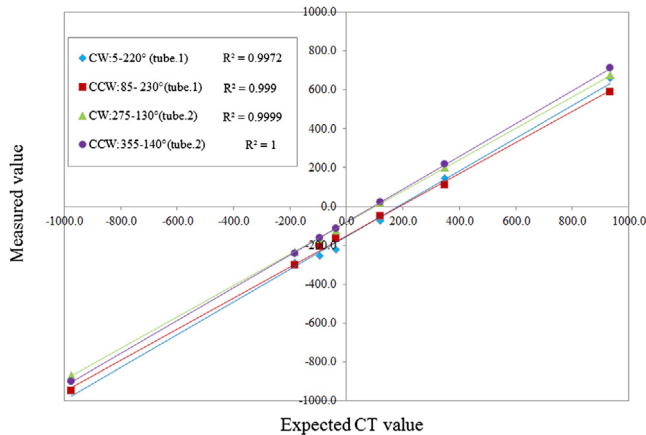


Fig. 3 – Comparison between the expected CT numbers and measured values for four conditions. CW refers to clockwise orientation, CCW counterclockwise orientation and R^2 is the determination coefficient.

Fig. 3 shows that the contrast materials were linearly related to known-values, with a coefficient of determination (R^2) higher than 0.997.

4. Discussions

In this work, the performance of the Vero4DRT system was characterized in terms of objective measurements of image geometric, image uniformity, high/low contrast resolutions, and contrast linearity. The comparison between the expected and measured distances of the four central markers of the Catphan phantom shows an excellent agreement. The CBCT for Vero4DRT system cannot perform a full 360° rotation, leading to a loss in uniformity for image acquisition. The main objective of the IGRT is to verify the target location around the isocenter. Therefore, the image quality at the periphery is not more important than the center region. In this study, the standard deviation at the ROI center is approximately 6.0HU. This value may be used for the CBCT image QA. The MTF does not depend on the rotation angle direction and tube, given that the high contrast is not affected by image noise. Chan et al. reported 11–12 Lp/cm in high-resolution mode using a full-circle scan for Varian CI-IX CBCT and Elekta XVI CBCT systems.⁶ Vero4DRT has a relatively smaller spatial resolution (8 Lp/cm) than the aforementioned systems. However, Vero4DRT has a relatively better spatial resolution than

Siemens Oncor MV CBCT and Tomotherapy Hi-Art Helical MV fan-beam CT systems (3–5 Lp/cm).⁶

Low contrast depends on image noise; thus, on tube rotation angles. Varian and Elekta CBCT systems can detect circles at 8 Lp/cm in 1% contrast (3-mm diameter),⁶ similar to our results. Varian OBI system showed only small differences (less than 10 HU) in density calibration between planning and CBCT, which makes it appropriate for treatment planning.¹⁷ The contrast linearity of Vero4DRT system is out of range as presented in the manufacturer manual. Vero4DRT system concept does not have adaptive radiotherapy treatment planning using CBCT. Additionally, some parts of the patient body are out of the FOV in the Vero4DRT system CBCT. Contrast linearity for Vero4DRT system presented a good relation with known-values. Therefore, we should check the contrast linearity.

5. Conclusion

In this study, we considered the CBCT image QA for Vero4DRT system. As the Vero4DRT system only perform a 215° rotation for image acquisition, we cannot perform image uniformity QA. High/low contrast QA can be visually checked, and we should check the contrast linearity compared with known value, even though it is out of range from the manufacturer manual.

Conflict of interest

None declared.

Financial disclosure

None declared.

REFERENCES

1. Fung AY, Enke CA, Ayyangar KM, et al. Prostate motion and isocenter adjustment from ultrasound-based localization during delivery of radiation therapy. *Int J Radiat Oncol Biol Phys* 2005;61(4):984–92.
2. Dawson LA, Jaffray DA. Advances in image-guided radiation therapy. *J Clin Oncol* 2007;25(8):938–46.
3. Paluska P, Hanus J, Sefrova J, et al. Utilization of cone-beam CT for offline evaluation of target volume coverage during prostate image-guided radiotherapy based on bony anatomy alignment. *Rep Pract Oncol Radiother* 2012;17:134–40.

4. Baker M, Behrens CF. Prostate displacement during transabdominal ultrasound image-guided radiotherapy assessed by real-time four-dimensional transperineal monitoring. *Acta Oncol* 2015;**54**(9):1508–14.
5. Kim Y, Li R, Na YH, et al. Accuracy of surface registration compared to conventional volumetric registration in patient positioning for head-and-neck radiotherapy: a simulation study using patient data. *Med Phys* 2014;**41**(12):121701.
6. Chan M, Yang J, Song Y, et al. Evaluation of imaging performance of major image guidance systems. *Biomed Imaging Interv J* 2011;**7**(2):e11.
7. Cheng HC, Wu VW, Liu ES, et al. Evaluation of radiation dose and image quality for the Varian cone beam computed tomography system. *Int J Radiat Oncol Biol Phys* 2011;**80**(1):291–300.
8. Stock M, Pasler M, Birkfellner W, et al. Image quality and stability of image-guided radiotherapy (IGRT) devices: a comparative study. *Radiother Oncol* 2009;**93**(1):1–7.
9. Klein EE, Hanley J, Bayouth J, et al. Task Group 142 Report: quality assurance of medical accelerators. *Med Phys* 2009;**36**(9):4197–242.
10. Kamino Y, Takayama K, Kokubo M, et al. Development of a four-dimensional image-guided radiotherapy system with a gimbaled X-ray head. *Int J Radiat Oncol Biol Phys* 2006;**66**(September (1)):271–8.
11. Kamino Y, Miura S, Kokubo M, et al. Development of an ultrasmall C-band linear accelerator guide for a four-dimensional image-guided radiotherapy system with a gimbaled X-ray head. *Med Phys* 2007;**34**(5):1797–808.
12. Nakamura M, Sawada A, Ishihara Y, et al. Dosimetric characterization of a multileaf collimator for a new four-dimensional image-guided radiotherapy system with a gimbaled X-ray head, MHI-TM2000. *Med Phys* 2010;**37**(9):4684–91.
13. Mukumoto N, Nakamura M, Sawada A, et al. Accuracy verification of infrared marker-based dynamic tumor-tracking irradiation using the gimbaled X-ray head of the Vero4DRT (MHI-TM2000). *Med Phys* 2013;**40**:041706.
14. Miyabe Y, Sawada A, Takayama K, et al. Positioning accuracy of a new image-guided radiotherapy system. *Med Phys* 2011;**38**(May (5)):2535–41.
15. The phantom laboratory. *Catphan 504 and manual*; 2013.
16. Droegge RT, Morin RL. A practical method to measure the MTF of CT scanners. *Med Phys* 1982;**9**:758–60.
17. Yoo S, Yin FF. Dosimetric feasibility of cone-beam CT-based treatment planning compared to CT-based treatment planning. *Int J Radiat Oncol Biol Phys* 2006;**66**:1553–61.